

**Final report for project entitled
"Tunable composite metamaterials with imbedded coherently controllable
atomic or molecular materials ",
under Grant no. AOARD – 094042
PI: S. Anantha Ramakrishna**

The **stated research goals** of the project were:

“The work will concentrate on the theoretical understanding of composite metamaterials at optical and near-infra-red frequencies by involving suitable atomic / molecular media in the construction the metamaterials designs that can be easily fabricated by conventional processes. Specifically,

1. Theoretical design of suitable coherently controllable metamaterials structures at optical and infra-red frequencies.
2. Engineering the bandwidths and bandstructures of metamaterials using atomic/molecular control.
3. Evaluate the performance of optically controlled switches made from controllable metamaterials for photonic applications. “

Achievements in the project:

Much of the work carried out under the project has been published in the following publications.

- Pub.[1] S. Chakrabarti, S. A. Ramakrishna, and H. Wanare, “Switching a plasmlike metamaterial via embedded resonant atoms exhibiting electromagnetically induced transparency”, *OPTICS LETTERS*, 34, 3728 (2009).
- Pub.[2] S. Chakrabarti, S. A. Ramakrishna, and H. Wanare “Controlling metamaterial resonances with light” *PHYSICAL REVIEW A* 82, 023810 (2010).
- Pub.[3] S. Chakrabarti and S. Anantha Ramakrishna, “Magnetic response of split-ring resonator metamaterials: from subwavelength structures to photonic bandgap structures”, *PRAMANA – JOURNAL OF PHYSICS*, (To be Submitted, 2010)

In this report, we will outline the work carried out, highlighting the results and referring to the publications (attached with the report) for the detailed calculations.

We will present the progress made and the results attained under each of the stated goals.

1. Theoretical design of suitable coherently controllable metamaterials structures at optical and infra-red frequencies.

Parametric control in three types of metamaterial structures were investigated:

1. Split resonator metamaterials that show effective magnetic activity
2. Dilute metallic wire structures that show plasma-like behaviour
3. Metamaterials made of plasmonic nanoparticles that show effective magnetic activity

In each case the field distributions, the level and ease of parametric control and the mechanism by which the control can be implemented turns out to be different, although the basic paradigm of parametric control by resonant processes in the imbedding material medium is the same. Further, we have obtained an important result that the control process is reasonably robust against the effects of dissipation as well as inhomogeneous broadening due to structuring defects.

In the first case of the split-ring resonator metamaterials, the large electric field amplitudes in the capacitive region can be taken great advantage by placing the coherent materials within the

Report Documentation Page

Form Approved
OMB No. 0704-0188

Public reporting burden for the collection of information is estimated to average 1 hour per response, including the time for reviewing instructions, searching existing data sources, gathering and maintaining the data needed, and completing and reviewing the collection of information. Send comments regarding this burden estimate or any other aspect of this collection of information, including suggestions for reducing this burden, to Washington Headquarters Services, Directorate for Information Operations and Reports, 1215 Jefferson Davis Highway, Suite 1204, Arlington VA 22202-4302. Respondents should be aware that notwithstanding any other provision of law, no person shall be subject to a penalty for failing to comply with a collection of information if it does not display a currently valid OMB control number.

1. REPORT DATE 07 OCT 2010		2. REPORT TYPE FInal		3. DATES COVERED 09-07-2009 to 08-07-2010	
4. TITLE AND SUBTITLE Tunable composite materials with imbedded coherently controllable atomic or molecular materials				5a. CONTRACT NUMBER FA23860914042	
				5b. GRANT NUMBER	
				5c. PROGRAM ELEMENT NUMBER	
6. AUTHOR(S) Anantha Ramakrishna				5d. PROJECT NUMBER	
				5e. TASK NUMBER	
				5f. WORK UNIT NUMBER	
7. PERFORMING ORGANIZATION NAME(S) AND ADDRESS(ES) Indian Institute of Technology, Kanpur, Office: 487, Faculty Building, Kanpur 208 016, India, IN, 208016				8. PERFORMING ORGANIZATION REPORT NUMBER N/A	
9. SPONSORING/MONITORING AGENCY NAME(S) AND ADDRESS(ES) AOARD, UNIT 45002, APO, AP, 96337-5002				10. SPONSOR/MONITOR'S ACRONYM(S) AOARD	
				11. SPONSOR/MONITOR'S REPORT NUMBER(S) AOARD-094042	
12. DISTRIBUTION/AVAILABILITY STATEMENT Approved for public release; distribution unlimited					
13. SUPPLEMENTARY NOTES					
14. ABSTRACT Research was conducted on the theoretical understanding of composite metamaterials at optical and near-infra-red frequencies by involving suitable atomic / molecular media in the construction the metamaterials designs that can be easily fabricated by conventional processes. Specific topics included 1. Theoretical design of suitable coherently controllable metamaterials structures at optical and infra-red frequencies. 2. Engineering the bandwidths and bandstructures of metamaterials using atomic/molecular control. 3. Evaluation of the performance of optically controlled switches made from controllable metamaterials for photonic applications.					
15. SUBJECT TERMS Metamaterials, composite materials, Optical Materials, Field Tunable Materials					
16. SECURITY CLASSIFICATION OF:			17. LIMITATION OF ABSTRACT Same as Report (SAR)	18. NUMBER OF PAGES 12	19a. NAME OF RESPONSIBLE PERSON
a. REPORT unclassified	b. ABSTRACT unclassified	c. THIS PAGE unclassified			

gaps. A full theoretical (analytic) description of the process of parametric control was developed. New resonances are shown to develop due to the interaction of the split ring resonator with the resonant dielectric material. Analytic expressions for the resonance frequencies, the widths of the resonances and the effective filling fractions were derived for the cases of the imbedding medium with Lorentz absorption and electromagnetically induced transparency (EIT). The details of the calculations can be found in Section 2 of Pub. [2].

We have addressed an important issue related to the practical design and manufacture of controllable metamaterials. This pertains to the inherent distribution in sizes that will happen in any fabrication process as well as increased dissipation that may result from material impurities and poor surface finish. It has been demonstrated in Pub. [2] that even though the effects are narrow-band, they survive inhomogeneous broadening effects, and the effects are also robust against increased dissipation. While the strength of the resonance decreases on the whole due to the larger effective filling fractions, the regions of reduced absorption between the resonances remain nearly unaltered. The “increased” filling fraction that remains unaffected by the inhomogeneous broadening compensates for the effect of the imperfections. In other words, the few resonant SRR units exhibit a large enough absorption cross section such that the reduced number of participating SRRs due to the inhomogeneous broadening does not adversely affect the response on average. Although accuracy in fabrication still remains an important issue, we note that the controllable effects discussed here are robust and generic to many metamaterials that depend upon resonances for their electromagnetic properties.

A detailed study of the evolution of the magnetic response of SRR metamaterials was carried out to understand the nature of the SRR resonance and the effects of photonic bandgaps on this resonant response. This was required because at high frequencies (Optical / NIR), the size of the SRR becomes comparable to the wavelength of light resonant with the structure. In this frequency regime, scattering effects become appreciable and significantly affect the response. It was found that at very high frequencies the SRR response becomes weak and Bragg scattering becomes dominant. However, at intermediate frequencies, the response of the SRR can be understood primarily as a resonant magnetic particle in spite of photonic bandgap effects. The table - 1 summarizes the interplay of these two effects. The details of the work can be found in Pub. [3].

Metallic nanowire meshes (dilute metals) that behave as plasmas can be made transmittive below the plasma frequency by imbedding in a resonant absorptive medium. Specifically, detailed calculations of this behaviour for silver nanowires imbedded in atomic sodium vapor have been carried out using realistic and experimentally obtained values for the material parameters of silver and sodium. Further, it has been demonstrated that this transmittive property can be controlled by an applied electromagnetic radiation (control field) that governs the behaviour of the imbedded Sodium. This is utilized for switching the metamaterial from a transmittive state to an opaque state or vice versa, depending on the wavelengths of the control and probe fields as well as the control field strength. This work has been published in Pub. [1]. We have confirmed these results with full three dimensional finite element calculations carried out by the COMSOLTM software acquired under this project. The field patterns show clearly that the theoretical basis involving volume averaged dielectric permittivity exactly describes this metamaterial as proposed by us in Pub. [1]. Some field patterns that are illustrative, at frequencies below and above the plasma frequency, are shown in Fig. 1.

Apart from sodium, we have found that Barium vapor and other similar metallic vapors can also be used for the control processes. More details about the different coherent materials is given in Section – 2.

Table 1. The changing nature of the response of the SRR whose structure has been shown in Fig. 1 as the gap width d varies.

SRR	Fig. no.	Gap width (nm)	Resonance (1) (THz)	Resonance (2) (THz)	Nature of resonance
(i)	Fig. 2	0	None	300	(1) None (2) Electric
(ii)	Fig. 2	4	138	326	(1) Magnetic, (2) Scattering
(iii)	Fig. 3	12	204	350	(1) Magnetic, (2) Scattering
(iv)	Fig. 3	20	238	370	(1) Magnetic, (2) Scattering
(v)	Fig. 4	44	304	400	(1) Magnetic, (2) Scattering
(vi)	Fig. 4	60	340	420	(1) Magnetic, (2) Scattering
(vii)	Fig. 5	76	370	447	(1) None, (2) Electric
(viii)	Fig. 5	124	None	466	(2) None, (2) Electric

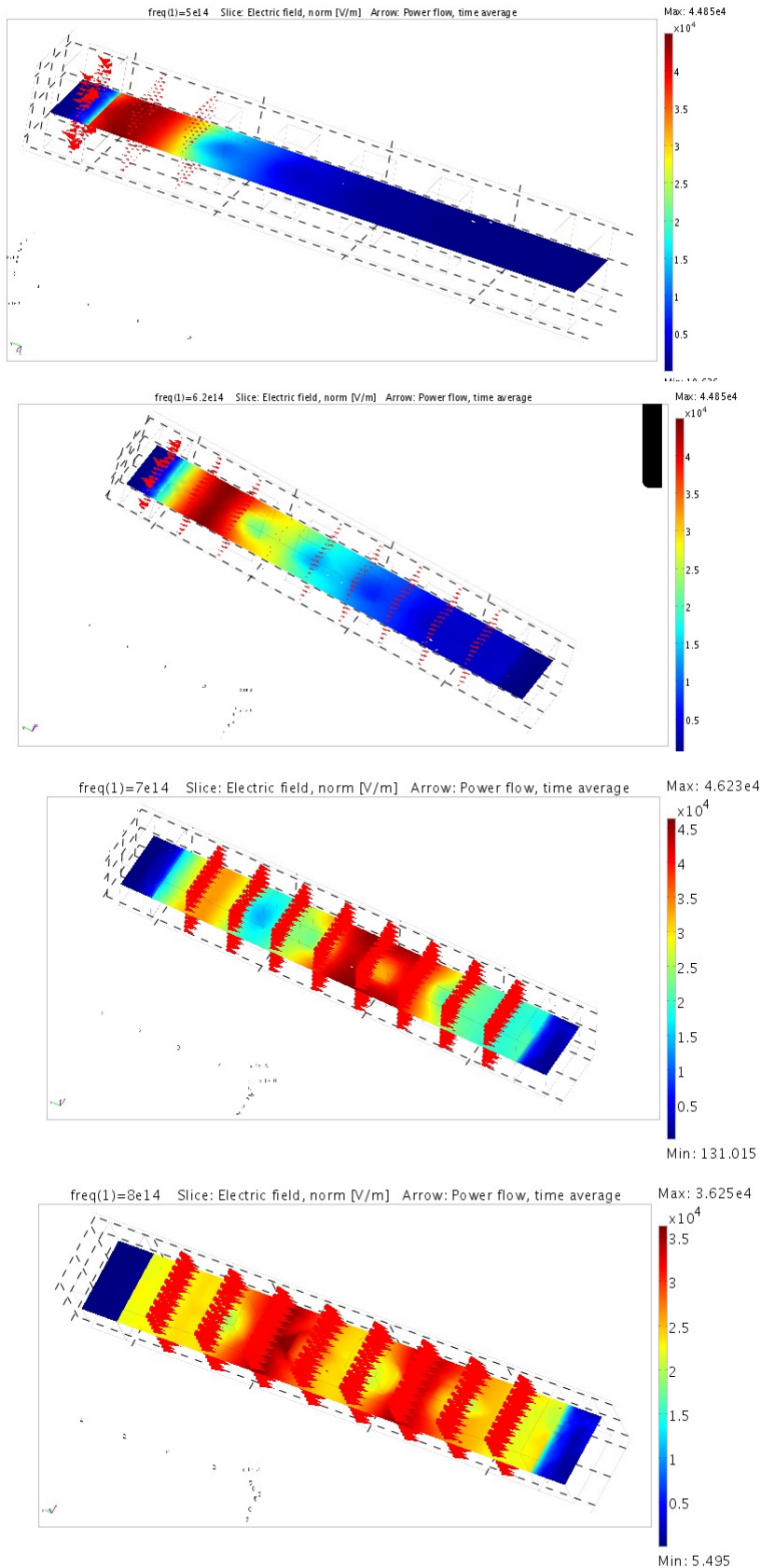


Fig. 1: Three dimensional field maps within a slab of a plasma-like metamaterial consisting of thin nanowires of silver corresponding to a filling fraction of about 17.4%. The wave is launched from the left and periodic boundary conditions are applied in the transverse directions. Perfectly matched layers at the two ends (left and right) ensure no fields exiting the slab do not reenter the system. No specific resonances are seen to be excited in the nanorods.

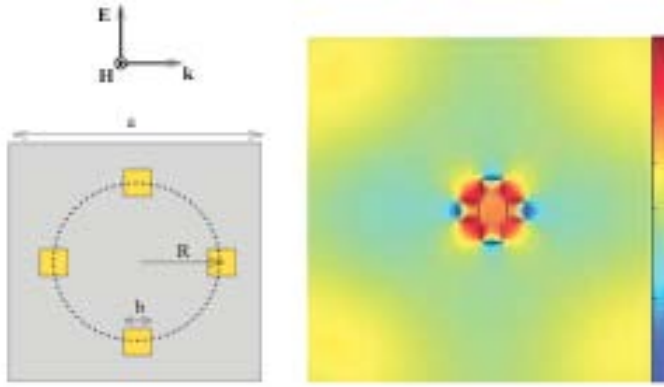


Fig. 2: Left panel: A cross-sectional view of a typical unit cell of the plasmonic loop metamaterial. The picture shows the nanorods placed on the circumference of a circle. The gray area represents the embedding dielectric medium. Right panel: Magnetic response of an isolated loop inclusion illustrating the concentration of the magnetic field inside the loop at resonance, when excited by means of a line source.

We have developed plasmonic loop magnetic materials which rely not only on their individual plasmonic resonance but also show magnetic activity that arises from the collective excitation. The plasmonic loop metamaterial consists of resonant plasmonic (metallic) particles arranged on a circular loop as shown in Fig. (2). The electromagnetic radiation with its magnetic field aligned along the axis of the loop drives this magnetic (plasmonic) collective resonance, if the frequency is close to the plasmonic resonance of the individual particles. We considered plasmonic rods and studied their photonic response and also the possibility of controlling the magnetic response parametrically by imbedding them in resonant media. Also note that the response of this medium is like a plasma for the other polarization with the electric field oriented along the axis of the rods. A detailed study of this resonance and the resonant

excitation of the magnetic resonance has been studied using the COMSOLTM software. The field maps reveals a concentration of the magnetic fields within the loop with the electric dipole moments of the individual particles oriented along the loop. The details of the metamaterial response are presented in Section 4 of Pub. [2].

By using the property that the plasmonic resonance frequency critically depends on the dielectric permittivity of the surrounding medium, we could develop schemes for control of this metamaterial. By controlling the dielectric permittivity of imbedding medium by coherent processes such as EIT medium like Barium vapors, one can switch the behaviour of the plasmonic loop metamaterial from a negative magnetic permeable medium to an absorptive positive magnetic medium. It has been considered that a metamaterial of silver nanorods imbedded in a optically nonlinear liquid such as carbon disulphide or amorphous silicon can be switched by using off-resonant Inverse Raman effects. The details of the control attained in this system is It is noted that the rod-like metamaterials considered here are already fabricated by electrodeposition processes using nanoporous alumina templates [G. Sauer, G. Brehm, and S. Schneider, "Highly ordered monocrystalline silver nanowire arrays" *J. Appl. Phys.* **91**, (2002)] and doping the alumina matrix using ion-beam implantation with the desired resonant atomic species is easily established as well.

Switching of this class of plasmonic resonant magnetic metamaterial composed of plasmonic nanorods (silver or gold) arranged on loops has been demonstrated. The negative magnetic bandgap is switched by changing the dielectric surroundings of the plasmonic particle using coherent processes such as resonant absorption or Inverse Raman absorption. It has been shown that the composite pumped metamaterial can be switched from a reflective state to an opaque state at frequencies within the bandgap region. Realistic, experimentally obtained parameters of silver, carbon disulphide and amorphous silicon have been used in this simulation.

In a related development, one of us have shown that it is possible to change and control the circular Bragg phenomenon in Chiral sculptured thin films by impermeating the porous structure with a Raman active liquid like CS₂ and using stimulated Raman Scattering into the Stokes modes.

Although this work was not directly supported by the project (and hence not acknowledged in the publication), we enclose the publication for details that may be useful for further development of this research.

2. Engineering the bandwidths and bandstructures of metamaterials using atomic/molecular control.

We have proposed a new paradigm of control, wherein the conventional metamaterial resonance is dressed by the properties of the background embedding material. Furthermore, a resonant response of the embedding material further transforms the composite metamaterial dramatically. We have shown a largely "capacitive" (Cut wires and plasmonic resonances [Pub.2]) and/or "inductive" (EIT based in [Pub.2]) control resulting in such composite metamaterials. On the other hand, we have also shown composite materials wherein the overall effect is akin to a volume averaged effect of the metamaterial and the embedding medium [Pub.1]. All these proposals rely on a carefully chosen background medium, whose intrinsic response offers some degree of control. Obviously there exist a range of materials as well as a range of electromagnetic phenomena that can be utilized for obtaining such resonant response. We have undertaken a wide study of a variety of materials with suitable atomic and molecular transitions that can be utilized for switching of composite metamaterials at optical and near-infra-red frequencies.

We have identified a few of them as extremely useful and interesting candidates that can be exploited for creating such composite metamaterials and also offer a fair degree of control of its resonant response. These materials have been identified keeping in mind their range of operation, operation characteristics as well as proper procedural issues related to embedding in solid matrix. We have earlier proposed the background species in such composite metamaterials to be atomic gases such as Na, Rb, Cs, Ba, He. These species provide a proof-of-principle system wherein the ideas of control of the composite materials is possible, however the actual large scale implementation in such a set up has its own limitation, as atomic vapour systems will involve isolating the metamaterial within a vacuum cell and the resulting bulky device. In order to realize compact systems we have focussed on systems where in the resonant species can be embedded in a solid matrix. The table below summarizes the most promising systems as the embedding background material for making composite media.

A detailed search for has been carried out. About a dozen transitions appear very promising for this purpose and we are studying these transitions. This list is given in the table below.

Table – 2: A list of promising transitions that can be used for parametric control of the metamaterials. The special features of these transitions are commented on in the last column.

Active Species	Host medium	Absorption		Emission		Reference	Comments
		Excitation	Width	Wavelength	Width		
Tetra-tert-butyl terrylene	Amorphous poly-iso butylene	567– 577 nm	2-3 MHz	Stoke Shifted by 20GHz	0.25, 0.5, 1.0, 2.5 @ various temp.	[1]	Single molecule spectra at 2, 4.5, 7, 16 K
1-(4-methyl phenyl)-3-(4-N,N, dimethyl amino phenyl)-2-propen-1-	Poly (methyl meth acrylate) PMMA	330-385nm 470-490nm 510-550nm.	20 nm	Blue Green Red		[2]	Solution casting technique for preparation Offers the possibility of Polychromatic emissions

one (MPDMA PP) chalcone derivative							
Azo dye doped polymer (ADP)	PMMA	236 nm (single photon) 785 nm 3-Photon 2-photon	150 nm Xe UV lamp + filter 36 nm	358 nm (strong) 591 nm (weak) 336 nm (Strong) 402 nm (weak)	60 nm	[3]	Ultra short pulse Ti: Sapphire laser (50 fs pulse at a repetition rate of 10 Hz @ 785nm) Using multi-photon excitation of the ADP- PMMA medium
Organic Laser dyes Rh.6G Rh.B K1	PMMA	470 nm 535 nm 560 nm	65 nm 55 nm 60 nm	-	-	[4]	Solar light concentrators Sunlight exposure UV absorption band of PMMA dominates below 300 nm
Four fluorene oligomers (Trimer, Pentamer, Heptamer, Polymer PFO)	Plastic Optical Fiber	300 to 600 nm	Pulsed Nitrogen laser (4 nsec pulse width, 10Hz, 470 micro-J/ pulse) Quartz tungsten Halogen lamp	Trimer 435 nm Pentamer 430 nm Heptamer 437 nm PFO 435 nm	30 nm 27 nm 38 nm 28 nm	[5]	Plastic Optical Fibers Oligomers concentration 0.02 % wt PFO 0.003% wt
Orange 11 dye 1-amino-2- methyl anthra quinone Disperse orange 11- DO11	PMMA Solid DMFM solution (di methyl form amide)	460 nm	Tungsten Halogen lamp Spectral range 200 – 1100 nm 100 nm	DO 11/PMMA 570 nm DO 11/DMFM solution 630 nm ASE 650 nm DO 11/PMMA	120 nm 40 nm 25 nm	[6]	Two gaussians peaks separated by ~ 100 nm Pumped at 532 nm Nd: YAG laser (20 micro- J/pulse) ASE (Amplified spontaneous emission) concentrations of 9 g/l pumped at 2 mJ/pulse
Er ³⁺	Poly methyl meth acrylate (PMMA)	2953 cm ⁻¹ 2994 cm ⁻¹	50 cm ⁻¹	Photo luminiscence 1540 nm	25 – 50 nm	[7]	At room temperature Er concentration varies from 0-20% Sample made by Spin coating on quartz/silicon substrate Excitation wavelength for PL was 980 nm
Eu ³⁺ ions in poly- crystalline powder Eu(fod) ₃ and also in Eu(fod) ₃	PMMA, poly- propylene (PP) and poly-	300 nm and/or 380 nm (absorption band starting at 15400 /cm)		PL spectra 17244 /cm (611 nm), 17261 /cm (614 nm)	1.5 nm sharp features	[8]	Temperature sensor PL quenching {Differential peak measurement for a good temperature sensor from using PL quenching }

(fod = 6,6,7,7,8,8,8-hepta fluoro-2,2-dimethyl-3,5-octane dionate)	dimethyl siloxane (PDMS)						
Eu(dbm)3(Phen), [Et4N] [Eu(ota)4] and Er(dbm)3(Phen),	Polymer thin films	300 – 400 nm PL kex = 350 nm	60 nm	PL spectra 612 nm (FWHM: 3.6 nm) 1534 nm (FWHM: 56 nm). 612 nm (FWHM: 5.25 nm)	3.6 nm 56 nm 5.25 nm	[9]	UV-processable fluorinated polymer material with high optical transparency across the visible and near infrared spectral range
fluorescein	boric-acid glass.	457.9 nm.	Ar-ion laser	490 nm	70nm	[10]	Single peak at 290 K Double peaked structure at 100 K separated by 77nm
Antimony oxide Sb-doped	soda-lime glass	295 nm	40 nm	371 nm	70 nm	[11]	Silver/sodium ion exchange (nanocrystal formation) can reduce this emission and induce a new peak at 615 nm, when irradiated with 395 nm light

References for Table -2:

[1] Low-Temperature Dynamics of Amorphous Polymers and Evolution over Time of Spectra of Single Impurity Molecules: I. Experiment

Yu. G. Vainer, A. V. Naumov, M. Bauer, and L. Kador
Optics and Spectroscopy, Vol. **94**, No. 6 (2003) 864–872

[2] Optical and Microstructural Studies on Chalcone Doped PMMA

V. Ravindrachary, S. D. Praveena, R. F. Bhajantri, Ismayil, J Seetharamappa, Vincent Crasta
International Conference on Advanced materials (ICAM 2009), Rio de Janeiro, Brazil, September (2009)

[3] Spectroscopic properties of azo-dye doped PMMA films studied by multi-photon absorption

Lisong Yang, Guiying Wang, Jianguang Wang, Guangbin Wang, Zhizhan Xu
Optik Vol. **113**, No. 4 (2002) 189–191

[4] Optical properties of some luminescent solar concentrators

M. A. EL-SHAHAWY and A. F. MANSOUR

Journal OF MATERIALS SCIENCE: MATERIALS IN ELECTRONICS Vol. **7** (1996) 171-174

[5] Spectroscopic Characterization of Plastic Optical Fibers Doped With Fluorene Oligomers

María Asunción Illarramendi, Joseba Zubia, Luca Bazzana, Gaizka Durana, Gotzon Aldabaldetrekue, and José Ramón Sarasua

JOURNAL OF LIGHTWAVE TECHNOLOGY, VOL. **27**, NO. 15, (2009) 3220

[6] Mechanisms of reversible photodegradation in disperse orange 11 dye doped in PMMA polymer

Natnael B. Embaye,^a Shiva K. Ramini,^b and Mark G. Kuzyk

THE JOURNAL OF CHEMICAL PHYSICS Vol. **129**, 054504 (2008)

[7] Optical Properties of Erbium and Erbium/Ytterbium Doped Polymethylmethacrylate
V. Prajzler, V. Jeřábek, O. Lyutakov, I. Hüttel, J. Špírková, V. Machovič, J. Oswald, D. Chvostová,
J. Zavadil
Acta Polytechnica Vol. **48**, No. 5, (2008) 14

[8] Optical properties of Eu(fod)₃-doped polymers using supercritical carbon dioxide
V.I. Gerasimova, Yu.S. Zavorotny, A.O. Rybaltovskii, A.Yu. Chebrova, N.L. Semenova, D.A.
Lemenovskii, Yu.L. Slovohtov
Journal of Luminescence Vol. **129** (2009) 1115–1119

[9] Optical properties of planar polymer waveguides doped with organo-lanthanide complexes
S. Moynihan, R. Van Deun, K. Binnemans, G. Redmond
Optical Materials **29** (2007) 1821–1830

[10] Enhancement of the nonlinear optical properties of fluorescein doped boric-acid glass through
cooling
Wayne R. Tompkin, Michelle S. Malcuit, and Robert W. Boyd
APPLIED OPTICS Vol. **29**, No. 27, (1990) 3921

[11] Optical properties of silver ion-exchanged antimony doped glass
S.E. Paje, M.A. Garcõa, M.A. Villegas, J. Llopis
Journal of Non-Crystalline Solids Vol. **278** (2000) 128

3. Evaluate the performance of optically controlled switches made from controllable metamaterials for photonic applications.

We evaluated the potential for optical switching of the controllable metamaterials by studying the frequency dependent transmittance / reflectance of slabs of the designed metamaterial in the absence and presence of control fields. We largely depended on numerical codes based on the transfer matrix methods for calculating the remittances for a plane wave incident on the slab. The metamaterials were considered to be made of silver which has the least dissipation at visible frequencies and the experimentally determined material parameters for silver [P. B. Johnson and R. W. Christy, “Optical Constants of the Noble Metals” Phys. Rev. B 6, 4370 - 4379 (1972)] were used as input to our numerical codes.

The requirements on the external stimulus for switching depend on the physical process used to exercise parametric control. The design of the metamaterial also influenced the extent to which the switching was possible. Since we typically investigated using atomic resonances with narrow bandwidths of 10-100 Mhz, the speed with which switching can be achieved would be on the time scales of only 10-100 nanoseconds. Thus, the switching speeds will be low here. We have, however, also tried using the inverse Raman effect for creating switchable absorptive conditions.

Typically, a metamaterial with only one of ϵ or μ at a given frequency would be highly reflecting as it does not permit any propagating waves within it. Hence, if the control process allows one to make the metamaterial attain positive material parameters in the presence of the pump, the metamaterial can be switched from a reflective to a transmittive state. One can also have switching from a transmittive state to a reflective state by choosing the structural and control parameters appropriately.

Switching with the three kinds of parametrically controllable metamaterials have been evaluated:

Resonant split ring resonator metamaterials: By imbedding the split ring resonators within a medium with a resonant absorption line controllable by an applied field (for example, using electromagnetically induced transparency) at frequencies within the bandgap arising due to

magnetic permeability, we can induce frequency bands of transparency. The Fig. 3 below shows the switchability for four layers of a split-ring resonators made of silver with a control field of about $10 \Omega_c$ (where Ω_c is the Rabi frequency). The total thickness of the slab is subwavelength (the SRR being subwavelength) and one can achieve transmission levels of almost 0.7 in the presence of the control laser while the transmittance is literally zero ($\sim 10^{-4}$) in the absence of the control field.

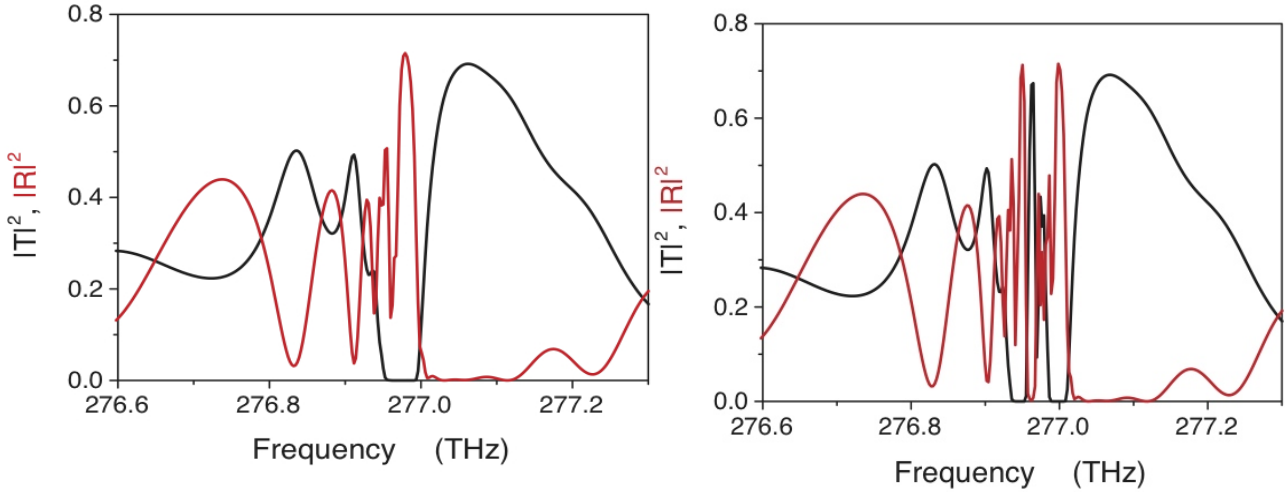


Fig. 3: Switching the response of a slab consisting of four layers of resonant split ring resonators by imbedding an atomic medium with a controllable resonant line within the bandgap. Possible atomic species at these frequencies are Eu^{3+} and Erbium. It can be seen that the absorption of the atomic species induces a transparency band within the negative magnetic bandgap (left panel). This can be further controlled by the application of a control field to create conditions of EIT for the atomic medium (Right panel). The narrow peaks are further controllable by the Fabry-Perot resonances of the slab. One can design for fine features in reflection and transmission.

Switchability of plasmalike metamaterials: By imbedding nano wire-structures, which have an effective plasmalike response at optical and NIR frequencies, within a resonant atomic medium with absorption lines below the plasma frequency, one can open up transmittive bands below the plasma frequency. This has been demonstrated by us using silver nanowires immersed within Sodium atomic gas, and the result for the D1 and D2 lines of Sodium is shown in Fig. 4. Since atomic species like Sodium are amenable for control using coherent processes like EIT, we checked this possibility and found that once again fine control of the transmittance is possible for a usually reflective metamaterial. The transmittance levels are not very high here and are about 0.3 to 0.4, but this should be sufficient for many device applications. This happens due to the absorptive and volume averaging nature of the metamaterial.

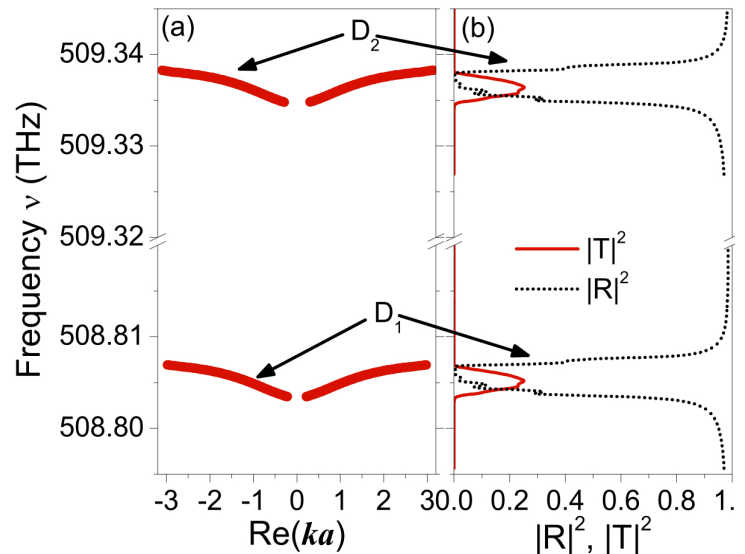


Fig. 4: Left panel: Band structure for s-polarized light with the metamaterial immersed in atomic sodium showing the new transmission band that develops below ω_p , for the Sodium D1 and D2 lines. Right panel: The reflectance and transmittance corresponding to the band structure on the left.

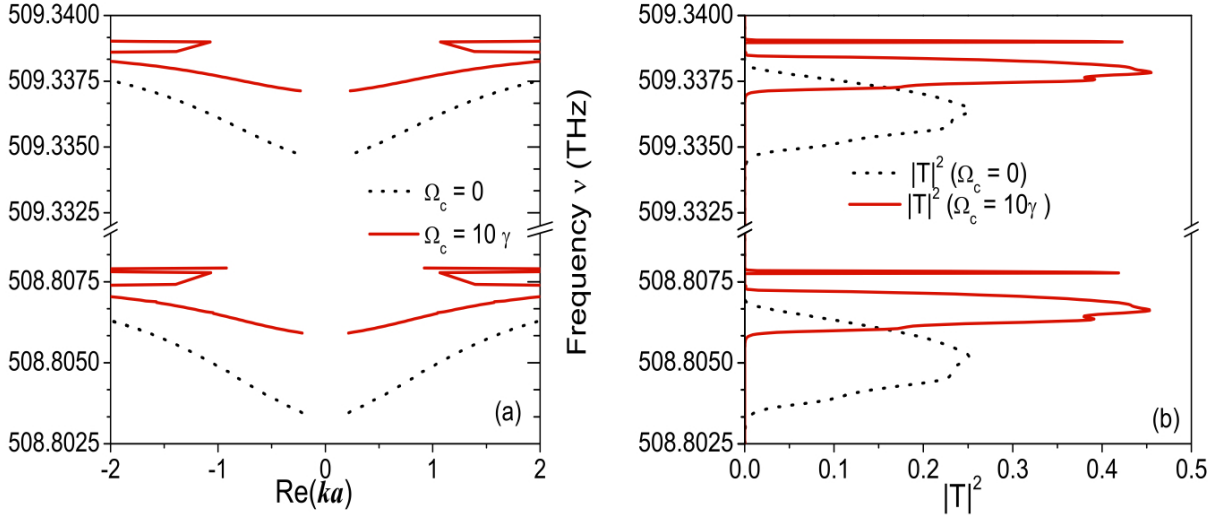


Fig. 5: Left: Band structure for s-polarized light with the metamaterial immersed in atomic sodium showing the new transmission band that develops below ω_p , for the D1 and D2 lines in the presence (solid) and in the absence (dotted) of an appropriate control field. Right: Transmittance corresponding to the band structure on left.

Switching with plasmonic loop metamaterials: Switching with plasmonic loop metamaterials was also investigated by us. We noticed that in this metamaterial, due to the complex and resonant nature of the plasmonic excitations, the level of the absorption was very large. Thus, while transmittance levels could be varied from 10^{-7} for the bare metamaterial to 10^{-3} in the presence of the control field, this was clearly insufficient for a device operation. However, we have noted that the medium state could be switched from a highly reflective for the bare medium to a less reflective state for the metamaterial imbedded with the coherent medium. As an example, we explored the possibility of switching using the inverse Raman effect that creates effective absorption at the Anti-Stokes frequency for an applied pump laser radiation. We chose the sizes of the plasmonic particles so that this frequency for control lies within the bandgap of the metamaterial. Thus, controllable switching from a reflective state to an absorptive state becomes possible with the application of the pump radiation. We show the change in reflectivity possible upon the application of a control field in a plasmonic ring metamaterial slab consisting of 4 layers of the plasmonic rings imbedded in CS_2 with and without the presence of a pump radiation with a typical intensity of about 100 GW/cm^2 . A change in reflectivity from about 35% to about 7% is apparent which is sufficient for many device applications. We also note that lower pump energies are possible by using other Raman active media such as amorphous silicon where similar effects are seen at few GW/cm^2 .

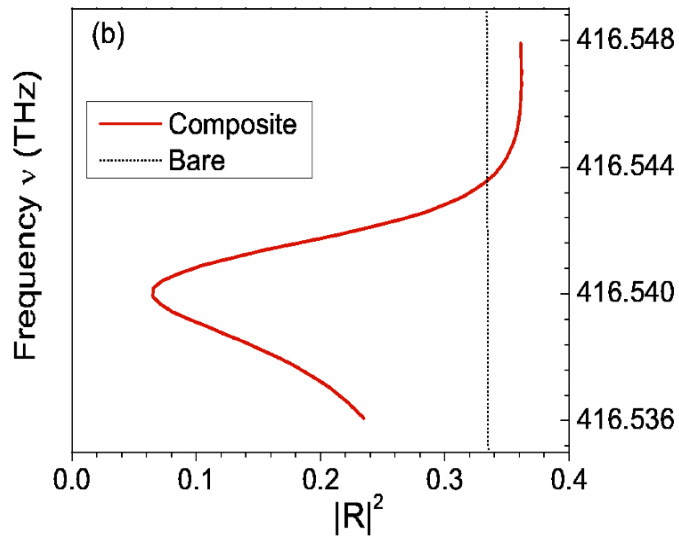


Fig. 6: The modified reflectivity of the plasmonic metamaterial in the neighborhood of a Raman transition in CS₂ (in which the metamaterial structures are immersed) at 416.54 THz. The vertical line represents the reflectivity of the bare metamaterial without the pump laser for the Raman transition.